Experimental investigation of the impact response of novel steel-biocomposite hybrid materials

Karthik Ram Ramakrishnan[1,*], *Mikko* Hokka[1], *Essi* Sarlin[1], *Mikko* Kanerva[1], *Reijo* Kouhia[1], and *Veli-Tapani* Kuokkala[1]

[1]Tampere University of Technology, Tampere 33720, Finland

Abstract. Recent developments in the production of technical flax fabrics allow the use of sustainable natural fibres to replace synthetic fibres in the manufacture of structural composite parts. Natural fibre reinforced biocomposites have been proven to satisfy design and structural integrity requirements but impact strength has been identified as one of their limitations. In this paper, hybridisation of the biocomposite with a metal layer has been investigated as a potential method to improve the impact resistance of natural fibre composites. The impact response of biocomposites made of flax-epoxy is investigated experimentally using a high velocity particle impactor. A high-speed camera setup was used to observe the rear surface of the plates during impact. Digital Image Correlation (DIC) of the high speed camera images was used for full-field strain measurement and to study the initiation and propagation of damage during the impact. The different modes of damage in the hybrid laminate were identified by post-impact analysis of the section of the damaged composite plate using optical microscopy. The study shows the difference in impact response for different material combinations and configurations. The hybrid construction was shown to improve the impact resistance of the flax composite.

1 Introduction

The feasibility of replacing traditional fibre reinforcements, specifically E-glass, with natural fibres such as from flax plant (*Linum usitatissimum*) has gained increasing attention due to their positive environmental profile as well as their low density. According to Shah et al. [1], the plant fibre reinforced polymers (PFRPs) are primarily used for non-structural applications such as in automotive interior components, and their potential as structural reinforcements is under-utilised. Pil et al. [2] reported that the use of natural fibres for high performance applications has been limited by a lack of data on the durability properties of these composites for loading conditions such as fatigue and impact. It has been reported that among different types of damages in a structure, e.g., fatigue, corrosion, and accidental impact damage, the most critical type of failure is impact damage, which will reduce the structural integrity rapidly and can lead to catastrophic failure. Impact loading can be caused by collisions between cars, cargo, maintenance damage, dropped tools (low velocity) or runway debris, hail, bird strike, and ballistic impact (high velocity). Therefore, it is essential to characterize the response of natural fibre composite structures to complex loading conditions, such as impact. Many researchers have studied the impact resistance of natural fibre reinforced composites. Bensadoun et al. [3] compared the impact resistance of different flax based composites and found that the thermoplastic composites outperformed the thermoset composites. Dhakal et al. [4] used an instrumented drop tower at low energies to characterise the damage performance of jute fibre reinforced unsaturated polyester composite for non-penetrating impacts. Santulli [5] developed a method to characterise the impact damage in flax-epoxy composites using hysteresis cycles. Scarponi et al. [6] studied the damage resistance and post-impact damage tolerance of plain weave hemp fabric reinforced bio-based epoxy composites subjected to low-velocity impact. Ramakrishnan et al. [7] studied the different modes of damage and the critical energy for complete penetration of flax-epoxy and flax-polypropylene composites using a combination of Digital Image Correlation and instrumented drop tower. Patel et al. [8] reported that the impact properties of the natural fibre composites were inferior to those of Glass Fibre Reinforced Polymers (GFRP), even after various optimisations, such as additional fillers and surface treatments. One of the proposed solutions to improve the mechanical properties of natural fibre composites for use in structural applications is hybridisation, either with synthetic fibres or with metals.

Hybrid structures combine two or more materials to produce lightweight materials with functional properties such as corrosion resistance, vibration damping and impact resistance. The synergistic effect of the hybrid materials produces desirable outcomes such as structural performance, reductions in energy consumption, and improved cost efficiency not achievable by constituent materials independently. For example, Zivkovic et al. [9] combined flax and basalt fibres in a hybrid composite

* Corresponding author: karthik.ramakrishnan@tut.fi

and showed that the hybrid construction can provide markedly improved impact behaviour in terms of damage mechanisms of dry and conditioned composite specimens. Fibre Metal Laminates (FML) are another class of hybrid composites that combine the superior fatigue and fracture characteristics of fibre reinforced composites with the plastic behaviour and durability offered by metallic materials. GLARE, a glass fibre-reinforced epoxy/ aluminium FML has been widely adopted in the aircraft industry and is currently used in the manufacture of the upper fuselage of the Airbus A380 aircraft. Reyes and Cantwell [10] showed that fibre metal laminates were capable of absorbing significant amounts of energy through plastic deformation of the aluminium. In addition, the breaking process of FMLs is a combination of metal-composite debonding, and failure in composite through fibre fracture, delamination and matrix cracking [11]. Frontan et al. [12] studied the ballistic resistance of carbon fibre and nano-crystalline steels and showed that the hybrids impacted on the composite side exhibit a higher energy absorption. Sarlin et al. [13] studied the impact resistance and fracture mechanisms of steel/composite hybrid structures and found that the use of rubber as a thin adhesive layer between stainless steel and composite can significantly reduce the damage area.

Although FMLs have been shown to be a successful hybrid solution in the case of glass and carbon fibre composites, there has been limited research investigating the properties of FMLs or metal-composite hybrids based on environment-friendly natural fibre composites. Kuan et al. [14] studied FMLs with aluminium and various natural fibres and found enhanced tensile and impact properties for the hybrid materials. Abdullah et al. [15] found a several-fold increase in the energy absorbed by Kenaf-Aluminium FMLs compared to Kenaf fibre composites. Wambua et al. [16] demonstrated a significant increase in the ballistic limit for a steel-flax hybrid material compared to flax composite and found that the energy absorbed by the hybrid material was even superior to mild steel. However, Santulli et al. [17] concluded that there were still many challenges with natural fibre metal laminates to obtain damage tolerance comparable to GLARE and identified non-optimal adhesion between the metal and FRP layers, especially for high-energy absorption, as a critical constraint.

In this paper, the dynamic mechanical properties of a novel hybrid material, in which a flax fibre-epoxy composite laminate is adhesively bonded to a steel layer, is investigated experimentally using a High Velocity Particle Impactor.

2 Materials and methods

The material chosen for the natural fibre reinforced biocomposite was a flax woven fabric supplied by Composites Evolution as Biotex Flax. The fabric was made of twistless natural flax fibres in a balanced 2x2-twill architecture with areal density of 400 g/m^2. Additionally, [0-90] plain woven ECR-glass fabric supplied by Ahlstrom-Munksjö with areal density of 400 g/m^2 was studied as a reference material. The chosen thermoset matrix was a two part epoxy resin supplied by Swiss composite (Araldite LY5052 epoxy resin and Araldur 5052 polyamine hardener). The resin and the hardener were mixed in the ratio of 100:38 by weight. A vacuum bagging system shown in Fig. 1 was used for the fabrication of the biocomposite and GFRP plates. The flax fabrics were dried at 60 °C for 24 h before the manufacturing process in order to minimize the moisture content. For the biocomposite, four plies of flax woven fabric were stacked and impregnated by 124.2 g of the epoxy resin/hardener mixture in a wet layup process before curing in a reusable vacuum bag. The laminated flax/epoxy composites were cured under vacuum of 0.75 bars at room temperature of 23 °C for 24 hours, followed by a post-curing of 15 hours at 50 °C in an oven. Eight plies of Glass fabric were used for the GFRP composite in a similar vacuum bag process. The average thickness of the cured composites were 3.1 mm and 2.2 mm for the flax-epoxy and glass-epoxy composites, respectively.

Though the composite laminates have different number of plies and thickness, they have similar mass of approximately 25 g for 80 x 80 mm square plate. The hybrid laminates were manufactured by adhesively bonding the composite laminate to 0.5 mm thick ferritic stainless steel supplied by Outokumpu Stainless Steel Oy. A commercial epoxy adhesive 3M™ Scotch-Weld™ epoxy adhesive paste DP460 was used to produce the steel/composite hybrid samples as this toughened adhesive exhibits good peel, shear and impact properties.

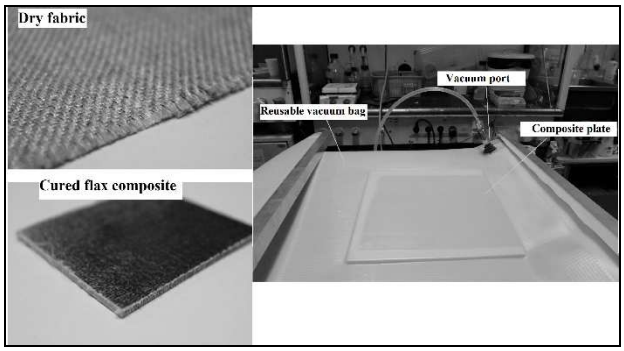

Fig. 1. Manufacturing of the flax fibre biocomposites using vacuum bagging.

2.1 Impact test device

The impact tests were carried out with an in-house built High Velocity Particle Impactor (HVPI). In this device, compressed air is used to fire a 9 mm diameter steel ball (2.98 g in weight) towards the target plate. A commercial ballistic chronograph was used to measure the velocity of the projectile, which can be changed by varying the launch pressure. The target plate with dimensions of 80 x 80 mm was clamped between two aluminium plates with a circular opening of 40 mm internal diameter in the centre, as shown in Fig. 2.

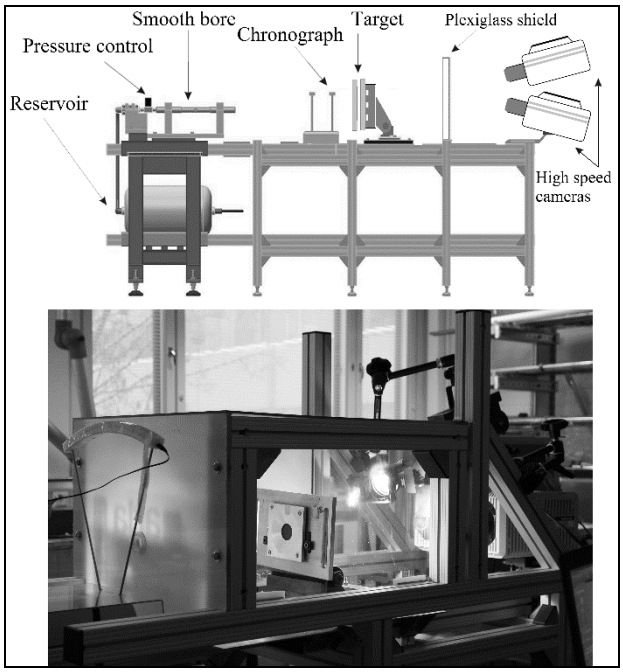

Fig. 2. Schematic picture of the HVPI device and a close-up of the target.

The rear surface of the target was observed during the impact with two high-speed cameras (Photron SA-X2) placed behind the target. The high-speed images were recorded at a constant frame rate of 120,000 fps and a resolution of 256 x 256 pixels. LaVision DaVis software was used for the acquisition and processing of the high speed camera images. A signal from the pressure control valve was used to trigger the image capture. The rear surface of the target plate was painted with a random pattern (white or black dots depending on the surface) to aid in the image correlation. The impact tests were conducted at a pressure of 3 bars, which corresponded to an initial velocity of 66 m/s measured by the chronograph. The kinetic energy of the projectile was 6.5 J. The tests included monolithic plates of steel, flax-epoxy, and glass-epoxy composites, as well as the Flax and GFRP - steel hybrid plates. The hybrid plates were tested in two configurations, i.e., impacted on the steel side or on the composite side. The nomenclature is such that the impacted side is named first; GFRP-Steel and Flax-Steel for impact on the composite side and Steel-GFRP and Steel-Flax for impact on the steel layer.

A typical series of images from the high speed camera is shown in Fig. 3. The images correspond to a 6.5 J impact on a flax-epoxy composite target. It can be seen that in the beginning of the impact, damage on the rear surface is clearly visible in the image 3(b). The area of the damage, which includes fibre failure, increases in subsequent images until in image 3(f) the steel ball is observed to fully penetrate the composite. The images are not at equal time intervals and are shown merely to illustrate the progression of damage in the composite. The duration of the impact, (time between the images 3(a) and 3(f)) was 0.275 milliseconds.

Digital image correlation (DIC) was conducted on the images obtained from the high speed cameras. DIC is based on the principle of comparing small zones (or subsets) of the digital images of the specimen surface

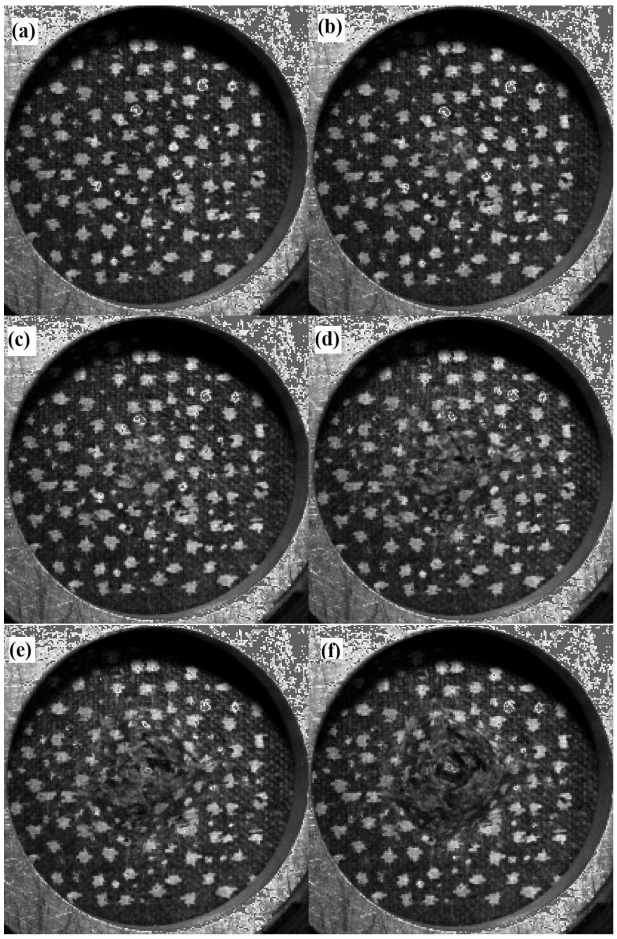

Fig. 3. Typical high-speed camera images of the impact loading of a flax composite with speckled pattern.

coated with a random pattern of high contrast speckles. A three-dimensional description of the target is achieved by the use of two high-speed cameras from two slightly different viewpoints. This allows stereo correlation to capture also the out-of-plane displacement caused by the impact. An image calibration procedure was conducted prior to the impact testing using 3D calibration plates provided by LaVision and the calibration parameters are fit using a pinhole camera model. The image correlation is performed by comparing subsets from the reference or undeformed sample and subsequent deformed states to directly provide full-field displacements and strains. It is therefore important to choose the correlation parameters to establish a reliable mechanical response of the material in the central zone near the point of impact. A square subset of size 25 x 25 pixels was chosen and the number of points to consider in the horizontal and vertical directions were defined by the number of step parameters (Ns= 6 pixels in x and y directions). The selection of the subset size was a balance between accuracy and resolution. In the stereo DIC, the in-plane displacement fields designated by u(x, y) and v(x, y) and the out-of-plane displacement w(x, y) correspond to the displacement that minimizes a similarity criterion between the reference and deformed subsets. The

Lagrangian strains are computed from the full-field displacement measurements.

3 Results and Discussion

The full-field displacement measurements obtained from the stereo-correlation were used to plot the waterfall plots of the progression of the z-displacement during the impact. In Fig. 4, the calculated displacement for 6.5 J impact on the steel side of a flax-steel hybrid laminate is shown for different time intervals during the loading cycle of the impact. A line across the diameter of the target plate was chosen for plotting the displacement profile. It can be seen that at Frame 1 corresponding to 8.3 microseconds, the beginning of the impact is visible as a small z-displacement. As the time increases, the displacement increases until t=100 μs, when the target has reached the maximum displacement of 2.2 mm. The plate is unloaded after this point and the z-displacement reduces. The advantage of the image correlation method is that we have the full field data and not just the central deflection. It is possible for the target to have the same peak deflection but completely different global response, (e.g., highly localised deformation and failure or global deflection of the plate and the shape of the crater). It should be noted that the centre of the plate (20 mm) does not correspond to the location of the peak displacement due to the trajectory of the projectile.

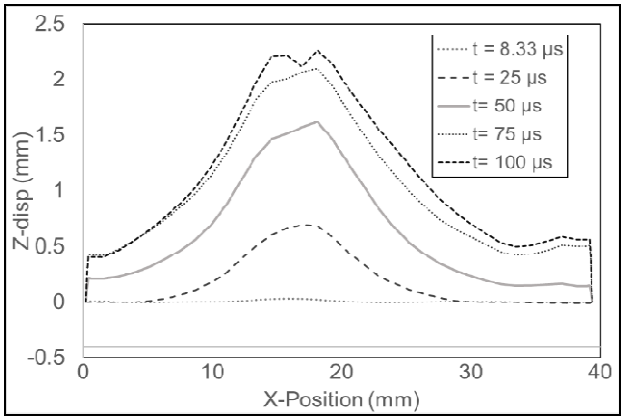

Fig. 4. Typical waterfall plot of the z-displacement for a flax-steel hybrid plate.

3.1 Impact of monolithic plates

The results of the impact tests on monolithic plates are summarised in Fig. 5. The front and rear surfaces of the steel, glass-epoxy and flax-epoxy plates impacted at the same energy exhibit markedly different responses. It can be seen that the steel plate shows large plastic deformation and the edge of the 40 mm diameter constrained area is visible. In the case of the GFRP plate, the region of the impact damage is clearly visible as a lighter region in the centre. The first modes of damage are typically matrix cracking and delamination. However, there is no evidence of perforation. In the case of the flax composite, there is a highly localised failure and complete perforation of the plate visible on both the impacted side and the rear surface.

The time history of the displacement at the centre of impact for the monolithic plates is also shown in Fig. 5. It can be seen that the total duration of the impact is between 0.2 and 0.3 milliseconds. The initial loading part of the curve up to 75 microseconds is very similar for the different plates. In the case of the steel plate, after the peak of 3.1 mm, there is a rebound of the plate but still a large residual displacement, confirmed by the plastically deformed plate in Fig. 5 (a). In the case of the GFRP plate, the rebound of the plate after the peak of 2.5 mm displacement is clearly evident and the displacement goes back to zero again. Due to perforation, the flax composite has a higher peak displacement compared to the steel and GFRP plates and the displacement continues to increase after the first peak of 3.6 mm. The dip in the displacement after the first peak corresponds to the time of the initiation of fibre failure in the rear surface. In reality, there is a small rebound of the impactor after 0.25 milliseconds, but it is not captured by the DIC system due to the perforation in the plate. The results of the impact on the monolithic plates indicate the need for hybrid construction to improve the impact response. In particular, for the flax composite, the hybrid material can prevent the perforation of the composite.

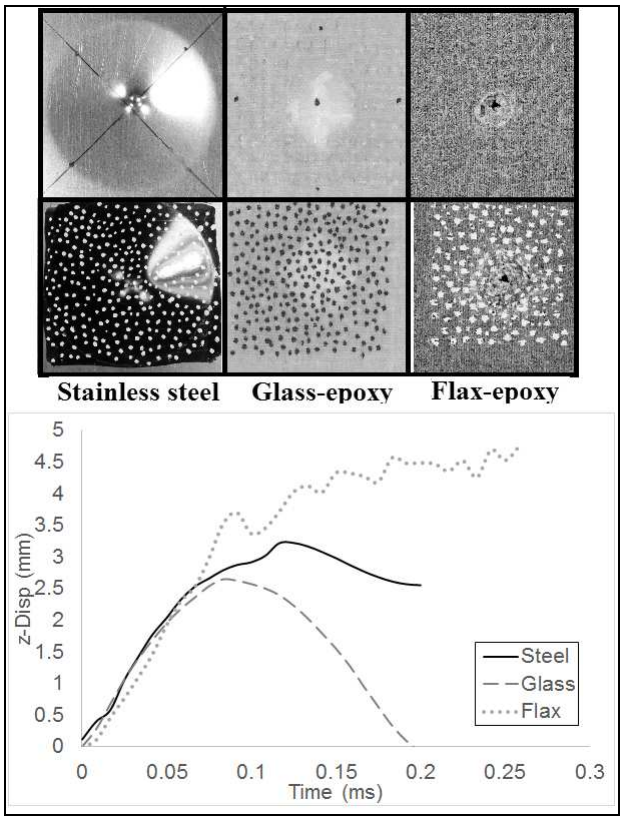

Fig. 5. (a) Front and rear surfaces after impact and (b) displacement-time history for steel, glass-epoxy, and flax-epoxy plates.

3.2 Impact of steel composite hybrid plates

The results of the impact tests conducted on the steel-composite hybrids are summarised. Fig. 6 shows the displacement-time history for the hybrid plates impacted on the composite side and on the steel side, respectively. It is clear from the plot that the duration of the impact has not changed significantly compared to the monolithic plates shown in Fig. 5. However, in all cases the peak displacement is significantly reduced. The highest displacement is for the steel-flax composite hybrid impacted on the steel side (2.2 mm). The image correlation was also able to measure the residual displacement observed in the GFRP-Steel hybrid.

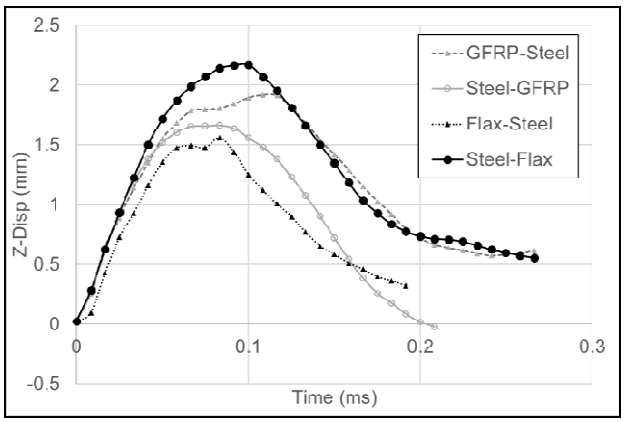

Fig. 6. Displacement-time history of the glass-epoxy and flax-epoxy – steel hybrid plates.

Fig. 7 shows the strain along the diameter of the target plate at peak displacement. It can be seen that the GFRP hybrid with the composite layer in the front experienced higher and more localised strain. This is mainly a result of the debonding between the composite and steel layers. However, when impacted on the steel side, there is a localised indentation on the steel layer but the load is dispersed over a larger area in the composite, as shown by the spreading of the strain history.

The same trend is not observed for the flax composite. In this case, there is more advantage to place the composite layer in front of the steel plate. The flax composite is weaker in tension and as a back layer there is evidence of fibre breakage in the principal fibre directions. The flax composite in the front shows some internal damage, but the Flax-Steel hybrid is closer to the GFRP-Steel in its strain history.

The cross-section of the glass and flax composite hybrid plates after the 6.5 J impact are shown in Fig. 8. The impacted plates were cut near the centre of the impact zone, and surface was embedded in an epoxy resin before grinding and polishing it for optical microscopy. It can be seen that the GFRP-Steel hybrid (impacted on the composite side) shows a large debonded zone between the composite and the metal. The steel layer, which is experiencing tension, undergoes plastic deformation similar to the monolithic steel plate, but not of the same magnitude. The GFRP layer shows considerable matrix failure and delamination between the plies of the composite. However, it is important to notice that the debonded zone of the steel layer shows some traces of the GFRP layer suggesting that the adhesive interface between steel and composite layers was strong. The same hybrid impacted on the steel side shows markedly different response. It can be seen that the steel layer is constrained by the GFRP layer and therefore does not have a global bending response but instead a more localised indentation. The GFRP back layer shows some signs of delamination and matrix cracking, but there appears to be no fibre failure or perforation.

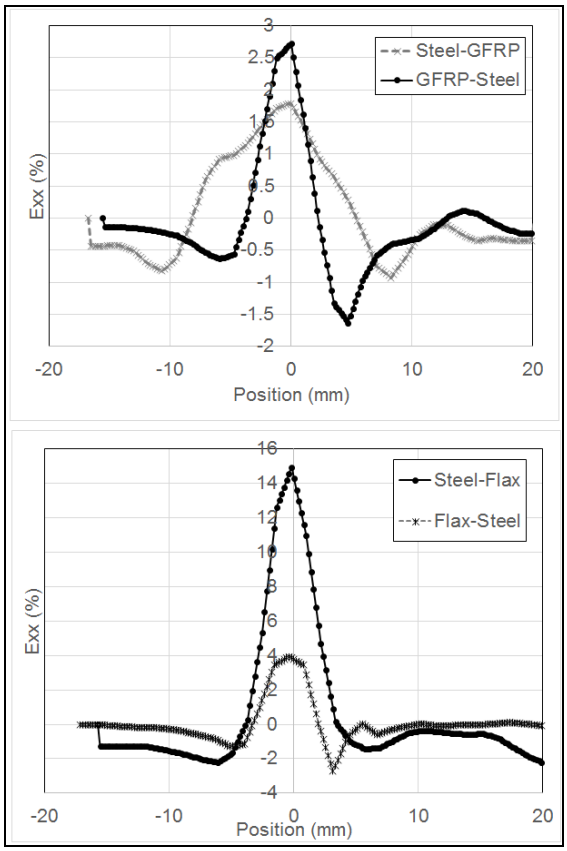

Fig. 7. Strain history of the glass-epoxy and flax-epoxy – steel hybrid plates.

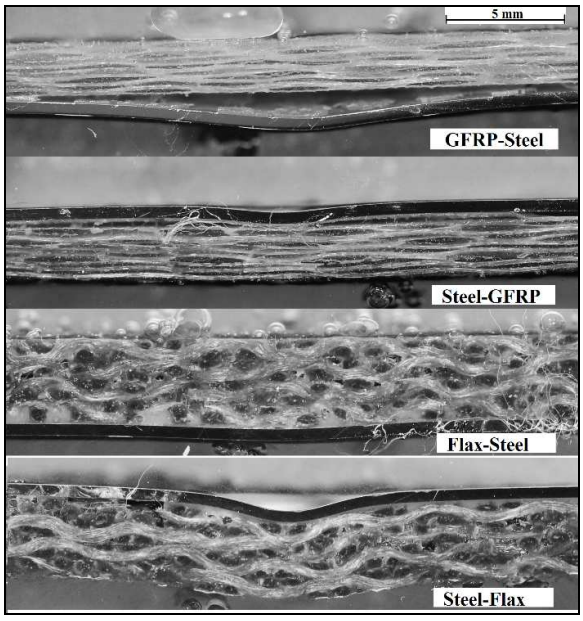

Fig. 8. Cross-section of GFRP and Flax hybrid composites.

In the case of the flax hybrid composites, it can be seen that the hybrid impacted on the steel side exhibits behaviour similar to the Steel-GFRP hybrid. The steel layer shows localised indentation but the depth of the indentation is much higher for the flax composite. In the composite layer, we can see some signs of fibre failure but delamination between the plies is not evident. This is not necessarily because the fibre-matrix interface is stronger for the natural fibre, but it is probably more an outcome of the structure of the flax composite, where the individual plies are not as separated as for the GFRP. An important finding is that the problem of perforation of the composite that was observed for the monolithic flax-epoxy plate can be avoided by the addition of the steel layer to the composite, irrespective of the direction of impact. However, further analysis is necessary to study in more details the damage resistance, energy absorption and residual strength of the hybrid composites.

Conclusions

The aim of this work was to investigate the impact response of environment friendly metal-composite hybrid materials made of adhesively bonded stainless steel and flax-epoxy composite layers. Traditional glass fibre composites were also studied as a reference material. An experimental campaign using a high velocity particle impactor was used to investigate the behaviour of these hybrid materials under medium velocity impact loading. A stereo digital image correlation system was used on images from two high-speed cameras observing the rear surface of the impacted target.

The failure mode in GFRP plates is predominantly matrix cracking and delamination, while the flax composite shows fibre failure and perforation. It was shown that the hybrid materials exhibit lower deformation compared to monolithic plates. An important aim of the impact tests was to investigate if there is a difference between the impact configurations with steel or composite layer in the front. It was shown that the placement of the flax composite layer on the impact side leads to different behaviour and failure modes compared to the case where the steel sheet acts as the front layer. The composite plate in front of the metal plate spreads the shock over a wider surface and can be an effective way to raise the relative energy absorption of the hybrid plate. This paper clearly shows the potential of hybrid constructions in improving the impact resistance of flax fibre composites, and will hopefully increase the adoption of natural fibre biocomposites in structural applications.

References

1. D. U. Shah, P. J. Schubel, and M. J. Clifford, *Compos. Part B Eng.*, vol. **52**, pp. 172–181 (2013)
2. L. Pil, F. Bensadoun, J. Pariset, and I. Verpoest, *Compos. Part A Appl. Sci. Manuf.*, vol. **83**, pp. 193–205 (2016)
3. F. Bensadoun, PhD Thesis, KU Leuven (2016)
4. H. N. Dhakal, V. Arumugam, A. Aswinraj, C. Santulli, Z. Y. Zhang, and A. Lopez-Arraiza, *Polym. Test.*, vol. **35**, pp. 10–19 (2014)
5. C. Santulli, vol. **36**, no. 1999, pp. 221–228, (2009)
6. C. Scarponi, F. Sarasini, J. Tirillò, L. Lampani, T. Valente, and P. Gaudenzi, *Compos. Part B Eng.*, vol. **91**, pp. 162–168 (2016)
7. K. Ramakrishnan, S. Corn, N. Le Moigne, and P. Slangen, *21st Intl. Conf. on Composite Materials*, August, pp. 20–25 (2017)
8. H. K. Patel, G. Ren, P. J. Hogg, and T. Peijs, *Plast. Rubber Compos.*, vol. **39**, no. 6, pp. 268–276 (2010)
9. I. Živković, C. Fragassa, A. Pavlović, and T. Brugo, *Compos. Part B Eng.*, vol. **111**, pp. 148–164 (2017)
10. G. Reyes and W. J. Cantwell, *Compos. Sci. Technol.*, vol. **60**, pp. 1085–1094 (2000)
11. T. Pärnänen, M. Kanerva, E. Sarlin, and O. Saarela, *Compos. Struct.*, vol. **119**, pp. 777–786 (2015)
12. J. Frontán, Y. Zhang, M. Dao, J. Lu, F. Gálvez, and A. Jérusalem, *Acta Mater.*, vol. **60**, no. 3, pp. 1353–1367 (2012)
13. E. Sarlin *et al.*, *Compos. Struct.*, vol. **108**, no. 1, pp. 886–893 (2014)
14. H. T. N. Kuan, W. J. Cantwell, M. a. Hazizan, and C. Santulli, *J. Reinf. Plast. Compos.*, vol. **30**, no. 6, pp. 499–508 (2011)
15. M. R. Abdullah, C. L. Pang, N. A. Husain, and B. Abdi, *Int. Rev. Mech. Eng.*, vol. **8**, no. 1, pp. 265–270 (2014)
16. P. Wambua, B. Vangrimde, S. Lomov, and I. Verpoest, *Compos. Struct.*, vol. **77**, no. 2, pp. 232–240 (2007)
17. C. Santulli, H. T. Kuan, F. Sarasini, I. De Rosa, and W. Cantwell, *J. Compos. Mater.*, vol. **47**, no. 18, pp. 2265–2274 (2013)